

1 **Reprogramming the transcriptional response to hypoxia with a chromosomally**
2 **encoded cyclic peptide HIF-1 inhibitor.**

3 Ishna N. Mistry¹ and Ali Tavassoli^{1,2,*}

4 ¹Chemistry, University of Southampton, Southampton, SO17 1BJ, UK.

5 ²Institute for Life Sciences, University of Southampton, Southampton, UK.

6 * e-mail: a.tavassoli@soton.ac.uk

7

8 **Keywords:** HIF-1, hypoxia, protein-protein interaction, cellular reprogramming, cyclic
9 peptide, SICLOPPS.

10

11 **Abstract**

12 The cellular response to hypoxia is orchestrated by HIF-1, a heterodimeric transcription factor
13 composed of an α and β subunit that enables cell survival under low oxygen conditions by
14 altering the transcription of over 300 genes. There is significant evidence that inhibition of
15 HIF-1 would be beneficial for cancer therapy. We recently reported a cyclic hexapeptide that
16 inhibits the HIF-1 α /HIF-1 β protein-protein interaction *in vitro* and prevents HIF-1-mediated
17 hypoxia-response signalling in cells. This cyclic peptide was identified from a library of 3.2 x
18 10⁶ members generated using SICLOPPS split-intein mediated protein splicing. With a view
19 to demonstrating the potential for encoding the production of a therapeutic agents in response
20 to a disease marker, we have engineered human cells with an additional chromosomal control
21 circuit that conditionally encodes the production of our cyclic peptide HIF-1 inhibitor. We
22 demonstrate the conditional production of our HIF-1 inhibitor in response to hypoxia, and its
23 inhibitory effect on HIF-1 dimerization and downstream hypoxia-response signalling. These
24 engineered cells are used to illustrate the synthetic lethality of inhibiting HIF-1 dimerization
25 and glycolysis in hypoxic cells. Our approach not only eliminates the need for the chemical
26 synthesis and targeted delivery of our HIF-1 inhibitor to cells, it also demonstrates the wider
27 possibility that the production machinery of other bioactive compounds may be incorporated
28 onto the chromosome of human cells. This work demonstrates the potential of sentinel
29 circuits that produce molecular modulators of cellular pathways in response to environmental,
30 or cellular disease stimuli.

31

32 **Introduction**

33 Transcription factors are master regulators of cellular fate and function that orchestrate a
34 coordinated response to a variety physiological stimuli. Exogenous modulation of
35 transcription factor activity therefore holds much therapeutic potential, and is a critical tool
36 for deciphering complex cellular networks. The absolute requirement of assembly for

37 function means that protein-protein interaction (PPI) inhibition is the optimal strategy for
38 intervention, but transcription factors are considered to be one of the most chemically
39 intractable targets in drug discovery.¹ More generally, the challenge of identifying PPI
40 inhibitors means that the majority of tools employed for studying these complexes are nucleic
41 acid-based (e.g. siRNA, or CRISPR) and function to eliminate the targeted protein from the
42 cell. Despite their widespread use, these methods have several drawbacks for studying PPIs;
43 removal of a protein from a system eliminates all of its known and unknown interactions and
44 functions. Thus an observed phenotype may not necessarily be attributed to a given PPI. In
45 cases where validated PPI inhibitors are available, the need for chemical synthesis and
46 intracellular delivery of such compounds places limitations on their adaptation and use. We
47 sought an alternative approach by introducing the components necessary to synthesize a PPI
48 inhibitor onto the genome of a human cell line. Under this scenario, the intracellular
49 production of a non-native molecule is selectively induced by one or more disease specific
50 signals via expression of the machinery needed for its production. This approach would have
51 the advantage that it eliminates the need for chemical synthesis and intracellular delivery of
52 the therapeutic agent. To demonstrate the viability of the proposed approach, we turned to our
53 recently reported cyclic peptide inhibitor of hypoxia inducible factor 1 (HIF-1)
54 heterodimerization.²

55 HIF-1 is a heterodimeric transcription factor that drives the cellular response to hypoxia,^{3, 4} by
56 altering the transcription of over 300 genes,⁵ enabling cell survival and growth in a low
57 oxygen microenvironment. HIF-1 is composed of an oxygen-regulated α -subunit (HIF-1 α)
58 and a constitutively expressed β -subunit (HIF-1 β). HIF-1 α is marked for degradation by
59 prolyl hydroxylases that use oxygen as a substrate.^{6, 7} Reduced oxygen levels lead to the
60 stabilization and nuclear translocation of HIF-1 α , where it binds HIF-1 β to form the active
61 HIF-1 transcription factor. HIF-1 α mounts an immediate response to reductions of
62 intracellular oxygen,⁸ while two closely related isoforms, HIF-2 α (also known as EPAS1) and
63 HIF-3 α , are thought to regulate the response to prolonged hypoxia.⁹ The intricate interplay
64 between HIF- α isoforms in cancer is complex and yet to be fully deciphered, but the role of
65 HIF-1 activity in angiogenesis, tumour growth and metastasis is well established.^{10, 11}

66 Tumours grow rapidly, outstripping the capacity of the local vasculature, which results in a
67 hypoxic microenvironment; HIF-1 α is overexpressed in many cancers,¹² and oncogene
68 activation and loss of tumour suppressor function is shown to be associated with HIF-1.¹³

69 We recently reported an inhibitor of the HIF-1 α /HIF-1 β PPI,² this molecule (*cyclo*-CLLFVY,
70 named P1) was identified from a genetically encoded library of 3.2 million cyclic
71 hexapeptides generated using split-intein circular ligation of peptides and proteins
72 (SICLOPPS).^{14, 15} P1 selectively binds to the PASB domain of HIF-1 α with a K_d of 124 nM,

73 disrupts the HIF-1 α /HIF-1 β PPI *in vitro* and in cells, and inhibits HIF-1 signalling in hypoxic
74 cells.² P1 is isoform-specific and does not bind to, or affect the function of the closely related
75 HIF-2 isoform *in vitro* or in cells.² SICLOPPS generated cyclic peptides via *Synechocystis sp*
76 PCC6803 (*Ssp*) DnaE split inteins;¹⁶ the SICLOPPS protein is composed of rearranged N-
77 terminal and C-terminal split inteins flanking a peptide extein sequence in the form of I_C-
78 extein-I_N. The N- and C-terminal split inteins combine to form an active intein that splices to
79 cyclize the extein (Figure S1A). By altering the sequence of the SICLOPPS extein at the
80 DNA level, a variety of cyclic peptides and proteins, including randomized cyclic peptide
81 libraries, may be produced by this approach.¹⁷
82 Given our goal of incorporating the machinery required for the generation of a molecular PPI
83 modulator into cells, and the significance of HIF-1 in tumour survival and growth, we set out
84 probe the possibility of engineering the conditional production of P1 (via the corresponding
85 SICLOPPS inteins) onto the chromosome of human HEK-293 cells, and to assess the effect
86 of genetically encoded P1 on HIF-1-mediated hypoxia response in these cells.

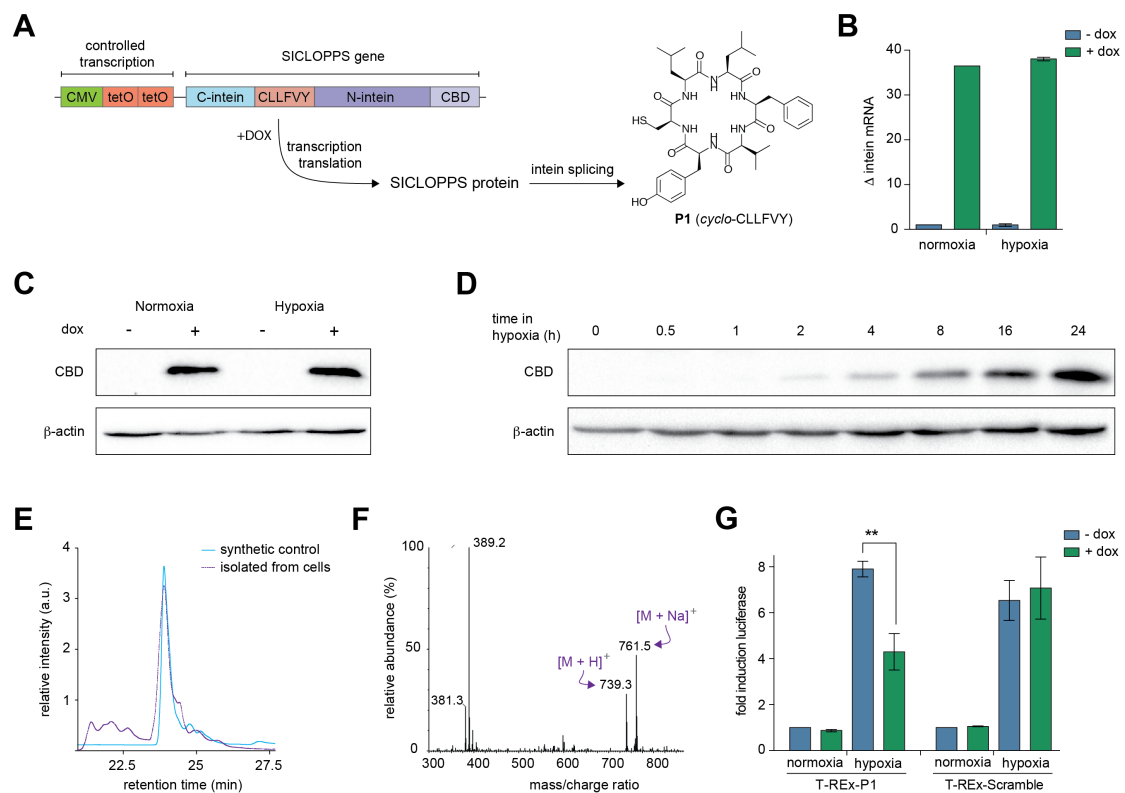
87

88 **Results**

89 Expression and processing of SICLOPPS constructs in HEK-293 cells

90 We began by constructing a cell line capable of conditional P1 production and assessing the
91 ability of the SICLOPPS construct to correctly function in human cells. To achieve inducible
92 expression of the SICLOPPS construct encoding our HIF-1 inhibitor, we used a cassette
93 containing a CMV promoter, followed by two copies of the tetracycline operator (tetO),
94 enabling regulation of transcription with doxycycline (dox), followed by the gene for
95 SICLOPPS (Figure 1A). Engineered *Nostoc punctiforme* DnaE (*Npu*) inteins that splice
96 significantly faster than the *Ssp* inteins typically used in SICLOPPS¹⁸⁻²⁰ were utilized for the
97 production of P1, with CLLFVY as the extein to be cyclized. We used flippase-flippase
98 recognition target (Flp-FRT) recombination²¹ to stably integrate this cassette onto the
99 chromosome of human HEK-293 cells (T-REx-293) to give T-REx-P1 cells. We first sought
100 to demonstrate the production of functional P1 from the chromosome of human cells. Intein
101 production was probed by immunoblotting with an antibody against the chitin-binding
102 domain (CBD) present on the C-terminus of the N-terminal intein; we only observed the CBD
103 band in the integrated cells, and only when cultured with dox (Figure S2A). The change in
104 transcription of the chromosomal SICLOPPS construct in response to dox was quantified by
105 RT-qPCR as ~37-fold in both normoxia and hypoxia (Figure 1B), which was also reflected at
106 the protein level (Figure 1C). A time course measuring intein protein production over 24 h in
107 hypoxic cells illustrated the steady build-up of SICLOPPS inteins (Figure 1D). The splicing
108 efficiency of the SICLOPPS protein encoding P1 was measured by immunoblot analysis for
109 the CBD. We only observed a single band at ~18 kDa corresponding to the spliced N-intein,

110 suggesting full splicing of the SICLOPPS protein (Figure S2B). We next sought to directly
 111 detect the presence of P1 in T-REx-P1 cells. A synthetic sample of P1 was prepared as a
 112 standard, and a peak with identical retention time as this sample was observed in the lysate of
 113 T-REx-P1 cells treated with dox (Figure 1E). Mass spectrometric analysis of this fraction
 114 from the cell lysate revealed peaks corresponding to the mass of P1 (Figure 1F) and the same
 115 as observed for the synthetic standard (Figure S3). This data demonstrates that the *Npu*
 116 SICLOPPS inteins incorporated into the chromosome of human HEK-293 cells are
 117 selectively produced in the presence of dox, splicing post translation to give detectable levels
 118 of P1 in the engineered human cell line.



119
 120 **Figure 1. Production of a functional cyclic peptide HIF-1 inhibitor from the**
 121 **chromosome of human HEK-293 cells.** (A) The chromosomally-integrated cassette enables
 122 the conditional expression of the SICLOPPS gene, which encodes the *Npu* inteins with
 123 CLLFVY as the extein. Splicing of these inteins gives P1. (B) RT-qPCR of intein expression
 124 in T-REx-P1 cells incubated in normoxia or hypoxia (24 h). (C) Immunoblot of T-REx-293
 125 and T-REx-P1 cells treated as in B (D) Immunoblot of T-REx-HRE cells incubated with dox
 126 in hypoxia for 0-24 h (E) P1 produced in T-REx-P1 cells has the identical HPLC retention
 127 time as the synthetic standard. (F) The mass spectrum (ESI+) of fraction shown in F from T-
 128 REx-P1 cell lysate shows the presence of P1. (G) Firefly luciferase activity in T-REx-P1 and
 129 T-REx-Scram cells transfected with a TK-HRE-luciferase and incubated for under normoxia
 130 or hypoxia (16 h). Data are means (n=3) ± SEM, **p < 0.01.

131

132 Genetically encoded P1 inhibits HIF-1 activity

133 With the engineered cell line in hand and having demonstrated the conditional production of
134 P1, the functionality of the genetically encoded cyclic peptide HIF-1 inhibitor was next
135 probed. T-REx-P1 cells were transfected with a HIF-dependent luciferase reporter plasmid,
136 where activation of HIF results in increased luciferase expression.²² As expected, there was
137 no change in the luciferase signal with dox in normoxia, while an ~8-fold increase in
138 luciferase activity was observed in hypoxic T-REx-P1 cells without dox (Figure 1G).
139 Induction of P1 production with dox in these cells resulted in a 50% decrease in luciferase
140 activity (Figure 1G), suggesting that chromosomally encoded P1 inhibits HIF-1 function. To
141 demonstrate that our observations are due to P1 and not the SICLOPPS inteins, we generated
142 a negative control cell line (T-REx-Scramble) that chromosomally encoded *cyclo*-CFVLYL
143 (a scrambled variant of P1) as the extein of *Npu* SICLOPPS inteins. Splicing and conditional
144 production of this scrambled peptide was demonstrated by immunoblotting (Figure S4). The
145 above luciferase assay was repeated in this cell line, and a ~7-fold increase in luciferase
146 activity was observed upon induction of hypoxia without dox. There was however, no change
147 in luciferase activity when these cells were incubated with dox in hypoxia (Figure 1G),
148 indicating that the scrambled peptide, or the SICLOPPS inteins do not affect HIF-1
149 dimerization. To validate that the effect from P1 was on HIF-1 rather than on luciferase, we
150 used a control SV40-luciferase plasmid, and did not see any significant change in luciferase
151 signal upon induction of P1 in T-REx-P1 cells with dox (Figure S5).
152 The effect of chromosomally produced P1 on HIF-1 activity was further assessed via its target
153 genes vascular endothelial growth factor (VEGF) and carbonic anhydrase IX (CAIX).
154 Chromosomally produced P1 reduced the VEGF transcription by ~30% (Figure S6A) and
155 CAIX transcription by ~45% (Figure S6B), with no effect of the scrambled peptide observed
156 on either gene (Figure S6). Together, the above data demonstrates that chromosomally
157 encoded P1 is functional, and able to inhibit HIF-1 signalling in hypoxia as expected from our
158 previous studies with the synthetic, tat-tagged variant of the compound.

159

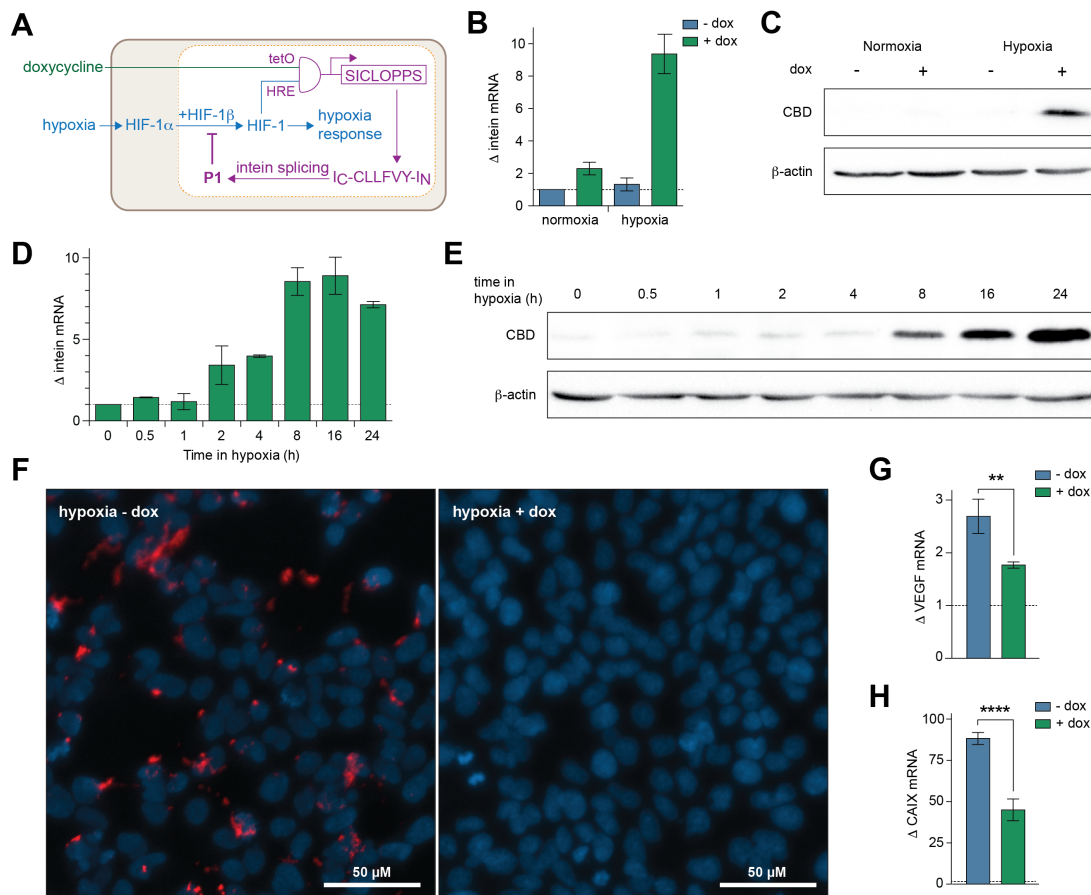
160 Engineering physiological control of peptide expression

161 We next sought to engineer an additional layer of control into the above system by limiting
162 the dox-dependent production of P1 to hypoxic cells. The motivation for constructing this
163 dual-control system was our long-term goal of generating an *in vivo* model that contains such
164 a circuit on its chromosome. Such a system would not only allow expression of the HIF-1
165 inhibitors in hypoxic tissues (as an HRE-only promoter would), but also allow temporal
166 control over initiation of P1 production via addition of dox. Thus the effect of HIF-1
167 inhibition at various stages of the tumour development may be assessed. A hybrid promoter
168 was designed and constructed; three copies of the HRE from the inducible nitric synthase

169 promoter²² were placed upstream of two copies of TetO, resulting in a dual physiological and
170 chemically controlled conditional promoter that would only function in hypoxia and with dox
171 (Figure 2A). This cassette was incorporated onto the chromosome of HEK-293 cells by Flp-
172 FRT recombination (as above) to give T-REx-HRE cells. Analysis of SICLOPPS cassette
173 transcription by RT-qPCR showed ~9-fold upregulated transcription in hypoxic cells that
174 were incubated with dox (Figure 2B). Immunoblot analysis showed the presence of
175 SICLOPPS protein only in cells cultured in hypoxia and with dox (Figure 2C), further
176 illustrating that the dual conditional promoter was functioning as designed. The quantity of
177 SICLOPPS protein was next compared with T-REx-P1 cells. Interestingly, we observed
178 higher levels of inteins in the CMV-promoted cell line than the HRE-promoted cells
179 incubated in hypoxia and with dox (Figure S7). Analysis of these bands by densitometry
180 indicated that there was ~7-fold more SICLOPPS intein in T-REx-P1 cells than in T-REx-
181 HRE cells after 24 h. There are two reasons for this difference; first, the transgene expression
182 rate from the HRE promoter is known to be lower than that from a CMV promoter,^{23, 24} and
183 second, the spliced product of the promoted protein (P1) is an inhibitor of HIF-1 dimerization.
184 Therefore, as P1 builds up, it will also inhibit the transcription factor promoting its own
185 production. To further assess the effect of this feedback loop on P1 production, a time course
186 analysis of intein production was conducted. We observed the steady build-up of SICLOPPS
187 mRNA (Figure 2D) and protein (Figure 2E) in hypoxic T-REx-HRE cells over 24 h, with a
188 noticeable increase in both after 8 hours in hypoxia.

189 The effect of P1 on the interaction of HIF-1 α and HIF-1 β in hypoxic T-REx-HRE cells was
190 next directly probed using an *in situ* proximity ligation assay (PLA).^{2, 25} A PLA signal was
191 observed in hypoxic T-REx-HRE cells incubated without dox (Figure 2F, left hand panel),
192 corresponding to the hypoxia-induced stabilization of HIF-1 α and subsequent dimerization of
193 HIF-1 α and HIF-1 β . The PLA signal was not observed in these cells when incubated with
194 dox (Figure 2F, right hand panel), nor in normoxic cells with or without dox (Figure S8). This
195 data demonstrates the disruption of HIF-1 dimerization by genetically encoded P1 in cells.

196 The downstream effect of disrupting HIF-1 dimerization with chromosomally encoded P1
197 was elucidated via analysis of the transcription of HIF-1 target genes VEGF and CAIX. The
198 expression of both genes was measured by RT-qPCR in cells incubated in hypoxia for 24 h
199 with or without dox. Induction of P1 with dox resulted in a ~40% reduction in VEGF mRNA
200 (Figure 2G) and a ~50% reduction in CAIX mRNA in hypoxic T-REx-HRE cells (Figure
201 2H). It should be noted that although lower amounts of the SICLOPPS protein are produced
202 in the T-REx-HRE cells than in T-REx-P1 cells, the extent of the effect of P1 on these HIF-1
203 reporter genes was similar in both cell lines, indicating that P1 concentration is not a limiting
204 factor in the observed inhibition of HIF-1 signalling.



205
 206 **Figure 2: Conditional production of P1 in human cells.** (A) The hybrid HRE/TetO
 207 promoter requires dual input signals of HIF-1 and dox in an AND process for expression of
 208 the SICLOPPS construct. Intein splicing produces P1, which inhibits HIF-1 dimerization. (B)
 209 RT-qPCR analysis of intein expression in T-REx-HRE cells incubated for 24 h in normoxia
 210 or hypoxia, with or without 1 μ g/mL dox. (C) Immunoblot of T-REx-HRE cells treated as in
 211 panel B. (D) RT-qPCR analysis of SICLOPPS mRNA levels in T-REx-HRE cells incubated
 212 in hypoxia for 0-24 h and treated with 1 μ g/mL dox. (E) Immunoblot for production of
 213 SICLOPPS protein over time. T-REx-HRE cells treated as in panel D. (F) PLA of T-REx-
 214 HRE cells treated with vehicle (left panel) or dox (right panel) and incubated in hypoxia for
 215 24 h. (G and H) RT-qPCR analysis of (G) VEGF and (H) CAIX expression in T-REx-HRE
 216 cells incubated in hypoxia for 24 h with or without 1 μ g/mL dox. Data are means (n=3) \pm
 217 SEM, **p < 0.01, ****p < 0.0001.

218

219 Endogenous P1 expression alters transcriptional response to hypoxia

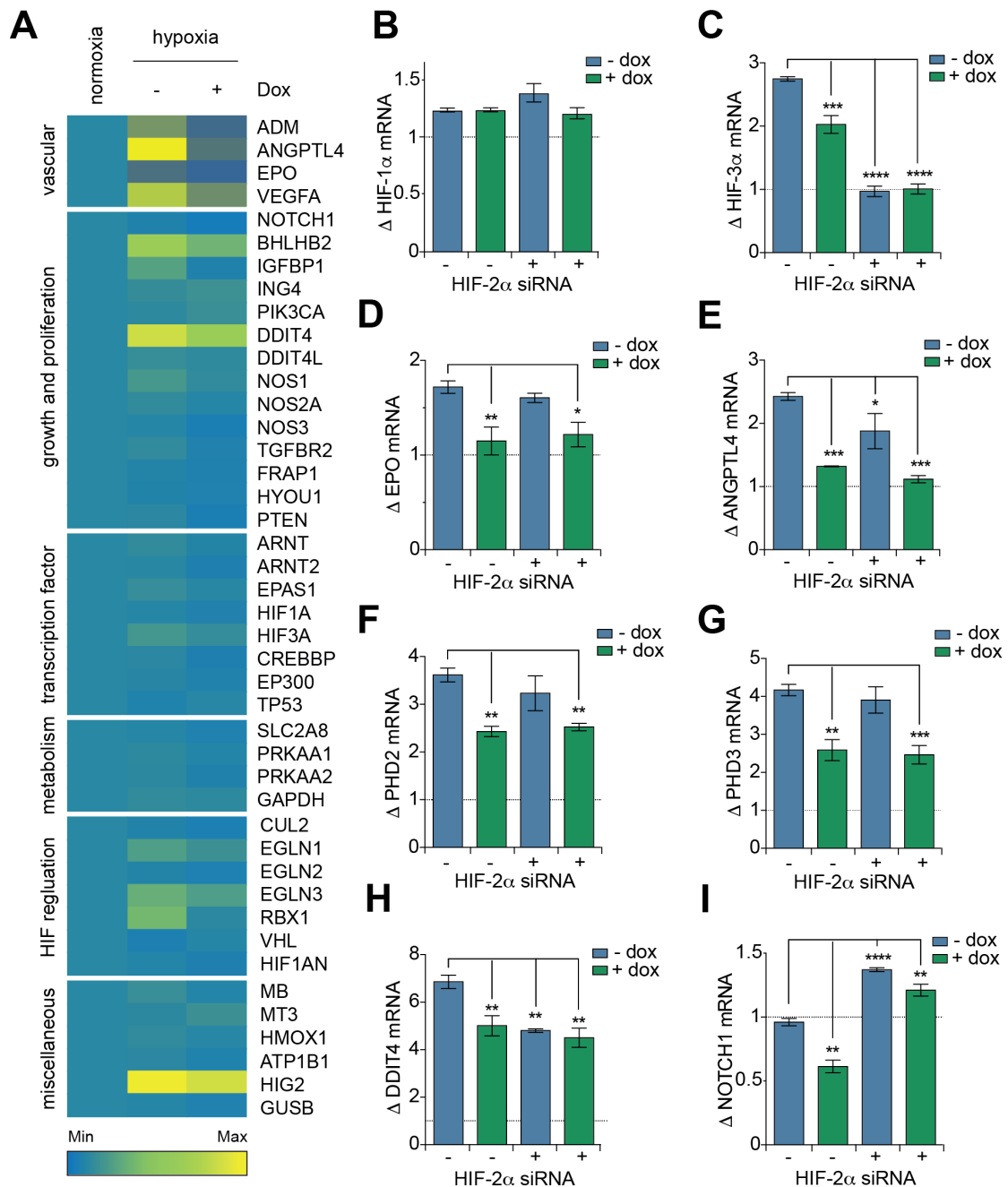
220 We broadened our analysis of the effect of P1 on HIF-1 signalling by using a focused
 221 microarray assessing expression of 43 hypoxia-associated genes (Table S1) in T-REx-HRE
 222 cells cultured in normoxia, hypoxia, and hypoxia with dox. The data showed altered
 223 expression of these genes in T-REx-HRE cells that were incubated in hypoxia with dox

224 (Figure 3A), illustrating the reprogramming of hypoxia response by P1 in these cells. We
225 have previously demonstrated (*in vitro* and in cells) that *cyclo*-CLLFVY is a specific inhibitor
226 of HIF-1 dimerization that does not affect the interaction of HIF-2 α and HIF-1 β .² We
227 therefore aimed to illustrate the potential of using genetically encoded P1 to separate the
228 effect of HIF-1 inhibition on hypoxia signalling from that of the closely related transcription
229 factor HIF-2. Our control experiments showed that treatment of T-REx-HRE cells with dox
230 had no effect on HIF-2 α mRNA levels (Figure S9A), and that siRNA knockdown of HIF-2 α
231 did not significantly affect the expression of HIF-1 α mRNA or protein (Figure S9B and S9C)
232 or SICLOPPS protein (Figure S9D).

233 The isoform-specificity of a number of HIF-target genes was next assessed using the above
234 approach. While there was no effect on HIF-1 α mRNA from either HIF-1 or HIF-2 (Figure
235 3B), HIF-3 α expression seemed to be primarily under the control of HIF-2 (Figure 3C). We
236 next assessed the role of HIF isoforms on genes involved in angiogenesis (ANGPT4 and
237 VEGF) and erythropoiesis (EPO). Following dox treatment, expression of EPO was
238 decreased to normoxic levels, whereas HIF-2 α siRNA treatment caused no significant
239 change, indicating EPO is a HIF-1 specific target (Figure 3D). In contrast, although inhibition
240 of HIF-1 significantly reduced the expression of ANGPT4 (Figure 3E) and VEGF (Figure
241 S9E), a combination of both dox and HIF-2 α siRNA treatments was required to reduce gene
242 expression to normoxic levels. This data suggests that expression of ANGPT4 and VEGF is
243 transactivated by both HIF-1 and HIF-2. Together, the inhibitory effect of P1 expression on
244 genes involved in the promotion of angiogenesis and erythropoiesis supports previous
245 assertions for the potential of targeting HIF-1 dimerization as a therapeutic strategy to prevent
246 tumour vascularisation.

247 Inhibition of HIF-1 dimerization and HIF-2 α siRNA treatment also differentially impacted
248 upstream effectors of oxygen-dependent regulation of HIF-1. Induction of P1 expression
249 resulted in a decrease in PHD2 and PHD3 mRNA whereas HIF-2 α siRNA has no significant
250 effect (Figure 3F and 3G). These observations are in line with the theory that HIF-1 mediates
251 the acute response to hypoxia whereas HIF-2 is the prominent driver of adaptation to
252 prolonged periods of hypoxic conditions.^{26, 27} Another gene primarily controlled by HIF-1
253 was CAIX, with no significant effect from HIF-2 α siRNA alone (Figure S9F). This data was
254 in agreement with reports of CAIX as a HIF-1 specific target.²⁸ Interestingly, although the
255 stress response gene DDIT4 was upregulated in hypoxia, and inhibition of HIF-1 and HIF-2
256 significantly reduced this induction, neither treatment was sufficient to reduce DDIT4
257 expression to normoxic levels (Figure 3H). DDIT4 is also induced in response to endoplasmic
258 reticulum stress and DNA damage related to the regulation of reactive oxygen species,^{29, 30}
259 which may be a result of hypoxic exposure, particularly when HIF response pathways are

260 disrupted.³⁰ Another gene of note was NOTCH-1, whose expression was halved in hypoxic
 261 cells treated with dox, but doubled in hypoxic cells treated with HIF-2 α siRNA (Figure 3I),
 262 illustrating the opposing regulatory roles of HIF-1 and HIF-2 on this gene. The above data not
 263 only demonstrates reprogramming of hypoxia response in our engineered human cell line, but
 264 also illustrates the potential utility of using genetically encoded P1, a HIF-1 specific inhibitor,
 265 to decipher the role of HIF isoforms in hypoxia signalling in a variety of cell lines.
 266



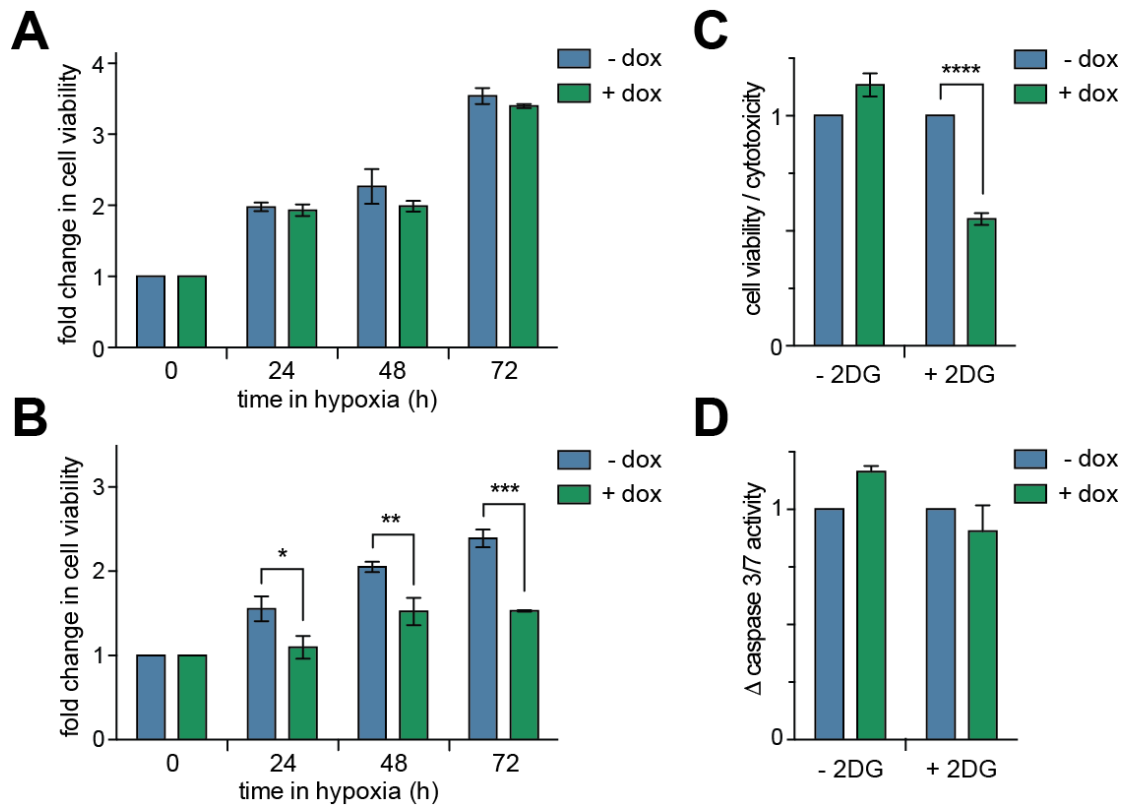
267
 268 **Figure 3. Expression of genetically encoded P1 alters the transcriptional profile of**
 269 **hypoxic HEK-293 cells. (A) Heat map of relative gene expression in T-REx-HRE cells**
 270 **transfected incubated in normoxia, or 24 h in hypoxia with or without 1 μ g/mL dox. Details**

271 of genes are given in Table S1. **(B-I)** RT-qPCR analysis of T-REx-HRE cells incubated in
272 normoxia, or 24 h in hypoxia with or without HIF-2 α siRNA, and with 1 μ g/mL dox with or
273 without HIF-2 α siRNA. Fold change in gene expression is shown relative to normoxic
274 expression (dotted line). Data are means (n=3) \pm SEM, **p < 0.01, ***p < 0.001, ****p <
275 0.0001.

276

277 Inhibition of HIF-1 dimerization confers synthetic lethality to glycolysis inhibitor

278 The effect on cell viability from the disruption of hypoxia-response signalling via inhibition
279 of the HIF-1 α /HIF-1 β PPI by P1 was next probed. The viability of T-REx-HRE cells cultured
280 in normoxia or hypoxia, with or without dox was assessed over 72 hours using 3-(4,5-
281 dimethylthiazol-2-yl)-2,5-diphenyltetrazolium bromide (MTT). No difference was observed
282 in the viability of cells cultured with dox versus those that were not (Figure 4A and Figure
283 S10), indicating that inhibition of the HIF-1 α /HIF-1 β PPI in hypoxic HEK-293 cells does not
284 affect viability. Nonetheless, previous studies have shown that knockdown of HIF-1 α by
285 siRNA sensitizes cells to the glycolysis inhibitor 2-deoxyglucose (2DG), leading to
286 cytotoxicity.³¹ We questioned whether inhibition of HIF-1 α /HIF-1 β PPI with P1 would
287 render HEK-293 cells susceptible to 2DG. This was initially assessed using MTT assays as
288 above. We observed a 37% reduction in viability after 72 hours in hypoxic T-REx-HRE cells
289 incubated with dox (Figure 4B). This observation was further probed with a triplex assay that
290 uses protease biomarkers to assess viability, cytotoxicity and apoptosis.³² We observed a 45%
291 decrease in the ratio of viable to cytotoxic T-REx-HRE cells after 72 h (Figure 4C), in line
292 with our observations from the MTT assay. Interestingly, no significant increase in caspase-
293 3/7 activity was observed in these cells (Figure 4D), suggesting that the observed synthetic
294 lethality of 2DG combined with P1 is not driven by apoptosis.³³



295

296

297

298

299

300

301

302

303

304

305

306

307

308

309

310

311

312

313

314

Figure 4. Assessing the effect of HIF-1 inhibition on T-REx-HRE cell viability. (A) Cells were incubated in hypoxia for up to 72 hours with or without 1 $\mu\text{g}/\text{mL}$ dox. Cell viability was assessed with an MTT assay. (B) Cells were treated as in panel A with or without the addition of 3 mg/mL 2DG to the culture media. (C) Cells were treated as in panel B and incubated in hypoxia for 72 h. The ratio of cell viability to cytotoxicity was determined using a triplex reporter assay. (D) Cells were treated as in panel C and apoptotic cell death was assessed via a caspase 3/7 activity assay. Data are means ($n=3$) \pm SEM, * $p < 0.05$, ** $p < 0.01$, *** $p < 0.001$, **** $p < 0.0001$.

Discussion

The conditional production of P1, an inhibitor of the HIF-1 α /HIF-1 β PPI, has been encoded onto the chromosome of a human cell line, and demonstrated to be a viable approach for the inhibition of HIF-1 signalling. Two versions of this sentinel circuit are reported, one that initiates P1 production in response to a chemical trigger (doxycycline), and a second that requires an environmental signal (hypoxia) in addition to doxycycline. In addition, the synthetic lethality of HIF-1 dimerization inhibition (by P1) and inhibition of glycolysis (with 2DG) is demonstrated. There is a growing body of evidence that inhibition of HIF-1, or re-direction of cellular pathways away from HIF-1 controlled mechanisms, may improve the anticancer effects of current chemotherapeutic agents.³⁴⁻³⁷ Using the T-REx-HRE cell line

315 reported here, a variety of chemotherapeutic agents may be screened for synthetic lethality, or
316 increased potency when combined with HIF-1 inhibition.^{38, 39}

317 This system has the potential to address several key questions about HIF-1 and its necessity
318 for the survival and growth of tumours. Since its discovery, a large body of evidence has
319 suggested that the HIF-1 transcription factor plays a significant and critical role in cancers,
320 enabling survival and adaptation in the hypoxic tumour microenvironment. However, recent
321 studies have indicated that HIF-1 α also functions in the cell as a monomer.⁴⁰⁻⁴² Approaches
322 that enable disruption of the HIF-1 transcription factor, without reducing the cellular level of
323 HIF-1 α have the potential to help decipher the role of HIF-1 in cancer. The sentinel circuit
324 reported above may, for example, be incorporated onto the genome of a variety of cancer cell
325 lines that are used in xenograft models. P1 production may be initiated at various points
326 during the tumour lifecycle, either globally or only within the hypoxic regions of the tumour,
327 illustrating the significance (or not) of HIF-1 as a target for cancer therapy. Another
328 possibility is the generation of *in vivo* models that contain the sentinel P1-encoding circuit on
329 their chromosome, enabling the effect of long-term HIF-1 inhibition on tumour formation and
330 maintenance to be studied; the dual control promoter limits P1 production to hypoxic cells
331 and allows temporal control over P1 production, enabling the study of HIF-1 inhibition at
332 various stages of the tumour lifecycle.

333 The concept of encoding the conditional production of a non-native small molecule from the
334 genome of engineered human cells has applications beyond the HIF-1 α /HIF-1 β inhibitor
335 described here. There are a multitude of natural products used as therapeutics that may be
336 hard-coded onto cells via their biosynthetic machinery, and produced as required. The use of
337 sentinel circuits to induce apoptosis in cells in response to specific DNA sequences,⁴³ or
338 encoding an environment-coupled kill-switch in bacteria⁴⁴ attests to the possibilities. Other
339 recent examples include the introduction of new biological components into cells for
340 therapeutic purposes.⁴⁵⁻⁵⁰ As the field of synthetic biology advances, such examples will grow
341 in number and complexity.

342

343 **Methods**

344 Cell culture

345 All cell culture reagents were purchased from Life Technologies unless otherwise stated. All
346 cells were cultured at 37°C in a humidified 5% CO₂ atmosphere. T-Rex-293 cells were
347 maintained in DMEM containing 10% fetal bovine serum (FBS), 100 μ g / mL zeocin and 15
348 μ g / mL blasticidin and integrated T-Rex cell lines were cultured in DMEM containing 10%
349 FBS, 100 μ g / mL hygromycin B and 15 μ g / mL blasticidin. Unless otherwise stated, T-REX
350 cells were dosed with 1 μ g / mL doxycycline (dox) to induce expression of integrated

351 constructs. Hypoxia treatment was achieved in a Don Whitley Scientific H35 Hypoxystation
352 with a humidified atmosphere containing 1% O₂ and 5% CO₂. Transfection of plasmids was
353 carried out using FuGENE HD (Promega) according to the manufacturer's instructions and
354 experiments were carried out 24 h after transfection.

355

356 Transfection and selection of stable clones

357 Stable mammalian expression cell lines were generated by Flp recombinase-mediated
358 integration. Flp-In T-REx-293 (T-REx-293) cells and plasmid vectors pcDNA5/FRT/TO and
359 pOG44 (the kind gift of Dr Noel Wortham) and are available commercially from Life
360 Technologies. pOG44 and pcDNA5/FRT vectors were transfected, at a ratio of 9:1, into T-
361 REx-293 cells with Fugene HD for the generation of stable cell lines. Polyclonal selection
362 was carried out with 200 µg/ mL hygromycin in high dilution culture. Integration was
363 confirmed by western immunoblotting.

364

365 Quantitative PCR

366 Total RNA was extracted from cells using ReliaPrep RNA Cell Miniprep System (Promega)
367 and quantified using a Nanodrop ND-1000 spectrophotometer. Complementary cDNA was
368 synthesized in a 20 µL reaction using 1 µg of total RNA with GoScript Reverse Transcriptase
369 (Promega) according to the manufacturer's instructions. Quantitative real-time PCR (RT-
370 qPCR) was performed using Universal Taqman PCR master mix (Applied Biosystems) and
371 the TaqMan gene expression assays of interest (Applied Biosystems) on a CFX-connect 96
372 Real-Time PCR system (Bio-Rad). Expression assays used in this study were: 18S
373 (Hs99999901_s1), ActB (Hs99999903_m1), VEGF (Hs00900055_m1), CAIX
374 (Hs00154208_m1), HIF-1α (Hs00153153_m1) and EPAS1 (Hs01026149_m1). Expression
375 values were expressed as $\Delta\Delta C_T$ normalized to expression of 18S and β-Actin and normoxic
376 gene expression. Hypoxia focused microarray was conducted using TaqMan Array Human
377 Hypoxia plates (Applied Biosystems). Expression values were expressed as $\Delta\Delta C_T$ normalized
378 to expression of 18S and normoxic gene expression.

379

380 Western Immunoblotting

381 For visualisation of expression of CBD tagged inteins, cells were lysed in intein extraction
382 buffer (20mM Tris.HCl, 1 mM TCEP, 0.5 mM NaCl, pH7.8) on ice for 15 minutes. For
383 visualisation of HIF-1α protein, cells were lysed by incubation on ice with
384 radioimmunoprecipitation assay buffer (50 mM Tris (pH 7.4), 150 µM NaCl, 1 mM EDTA,
385 1% v/v Triton X-100), and 1x protease inhibitor cocktail (Sigma) for 20 min.

386 Cell lysates were sonicated in an ice water bath then centrifuged at 10,000 rpm for 20 min at
387 4°C, and the protein concentration in the supernatant quantified by Bradford assay. Proteins
388 were separated on an SDS-PAGE gels (15% for CBD, 10 % for HIF-1 α), transferred to
389 PVDF membranes (Invitrogen) and subjected to immunoblot analysis. Mouse monoclonal
390 anti-CBD (E8034S, 1:250, New England Biolabs) anti-HIF-1 α (610958, 1:250 BD
391 Biosciences) were diluted in PBS containing 5% non-fat powdered milk and 0.1% Tween-20
392 and incubated with the membrane overnight at 4°C overnight. Horseradish peroxidase
393 conjugated anti-mouse antibody was used as the secondary antibody, and monoclonal anti-
394 β actin-peroxidase antibody (A3854, 1:100,000, Sigma) served as a loading control. Bound
395 immunocomplexes were detected using ECL primes western blot detection reagent
396 (RON2232, GE Healthcare) and analyzed using a ChemiDoc Imaging System (Bio-Rad) and
397 Image Lab 4.0 software (Bio-Rad).

398

399 Detection of peptide in cell lysates by HPLC and MS

400 T-REx-P1 cells were scraped in ice cold PBS and the cell pellet froze in N₂ (l). The pellet was
401 thawed and lysed in PMSF lysis buffer (5 mM EDTA, 2 mM EGTA, 0.4 mM PMSF in PBS)
402 containing protease inhibitor cocktail (sigma) by three freeze thaw cycles. 10 μ L of TFA was
403 added to precipitate proteins and the lysate centrifuged (8000 rpm, 30 min, 4°C). The
404 supernatant was passed through a 10 kDa cut off filter and the flow through collected and
405 analysed by reverse phase HPLC on a Waters HPLC system equipped with a Waters Atlantis
406 T3, Amide capped C18 5 μ m, 6 x 100 mm column. Samples were manually injected into a
407 Waters flex inject system into the HPLC system containing a Waters 1525 binary pump. One-
408 minute fractions were collected in the 5 minute window around the elution time of the
409 synthetic peptide and analysed by LC-MS.

410

411 HRE luciferase reporter assay

412 T-REx-P1, T-REx-Scramble, or T-REx-HRE cells were transiently transfected with a HIF
413 dependent firefly luciferase reporter construct (pGL2-TK-HRE) or a HIF independent firefly
414 luciferase reporter construct (pGL3-SV40) as a control. Transfected cells were incubated in
415 the presence or absence of 1 μ g/mL dox. After 24 h, cells were recovered and plated at
416 25,000 cells/ well in 96 well plates and incubated for 5 h before either hypoxic or aerobic
417 incubation for 16 h. Firefly luciferase activity was determined using Bright-Glo Reagent
418 (Promega) according to the manufacture's instructions. Luciferase signal was normalized
419 using the corresponding no-transfection controls for each plate.

420

421 Duolink proximity ligation assay

422 Duolink proximity ligation assay (PLA) was conducted using the in situ PLA Kit (O-Link
423 Bioscience, Uppsala, Sweden) according to the manufacturer's instructions. The antibodies
424 used were rabbit monoclonal anti-HIF-1 α (NB100-449, Novus Biologicals) and mouse
425 monoclonal anti-HIF-1 β (H00000405- B01P, Abnova). Cells were treated with 1 μ g/mL dox
426 in normoxia or hypoxia for 24 after which they were fixed with 2% formaldehyde in PBS for
427 10 min and permeabilized with 0.5% Triton (diluted in PBS) for 10 min. After pre-incubation
428 with the Duolink Blocking Reagent for 1 h, samples were incubated overnight with the
429 primary antibodies to HIF-1 α (1:500) and HIF-1 β (1:500). Duolink PLA probes and reagents
430 were added as recommended by the manufacture's instructions. Cells were imaged with a
431 fluorescent microscope (Zeiss Axio Vert.A1).

432

433 HIF-2 α knockdown

434 T-REx-HRE cells were seeded at 200,00 cells/well on 6-well plates and incubated for 24 h
435 such that cell density reached 50-70% confluence just prior to transfection with siRNA. Cells
436 were transfected with siRNA using Lipofectamine RNAiMAX transfection reagent (Life
437 Technologies) according to the manufacturer's instructions for 'forward transfection'. Briefly,
438 cell culture media was removed from cells and replaced with serum-free OptiMEM cell
439 culture medium (Life Technologies). siRNA and Lipofectamine were separately, diluted in a
440 volume of OptiMEM equivalent to 10% of the final volume of cells, and incubated at RT for
441 5 min. The diluted oligonucleotides and transfection reagent were then combined, mixed
442 gently, and incubated at RT for 10 min. The siRNA-Lipofectamine complexes were added
443 drop wise to cells which were then incubated at 37°C for 24 h. The final concentration of
444 siRNA was 5 nM and the final amount of Lipofectamine was 0.2% v/v for all experiments.
445 Cells were either transfected with EPAS1 (HIF-2 α) siRNA (Silencer Select pre-designed
446 annealed human oligonucleotide duplex, s4700, Life Technologies), scrambled siRNA
447 (Silencer Select negative control number 2, Life Technologies) or vehicle alone. Following
448 transfection, cells were incubated in hypoxic or aerobic conditions for 24 h in the presence or
449 absence of 1 μ g/mL for 24 h, then harvested for total RNA extraction.

450

451 Cell viability assays

452 T-REx-HRE cells were seeded in triplicate at 5,000 cells per well on 96 well plates 24 h prior
453 to dosing with 1 μ g/mL dox in 100 μ L fresh DMEM, DMEM without glucose or DMEM
454 containing 3 mg/mL 2-deoxy-glucose. MTT-based cell proliferation assays were performed
455 on untreated cells on the day of treatment or treated cells 24, 48 h or 72 h after treatment, as
456 follows: MTT (Sigma) was prepared in sterile PBS added to cells at a final concentration of 1
457 mM (10% v/v). Cells were then incubated at 37°C for 4 h until intracellular punctate purple

458 precipitated were clearly visible under the microscope. 75 μ L of the culture medium was the
459 removed from each well and 100 μ L DMSO added. The cells were incubated for 10 min in
460 the dark, with agitation to dissolve the insoluble formazan particles. Absorbance was
461 measured at 570 nm on a microplate reader (Tecan Infinite M200 Pro). ApoToxGlo assays
462 (Promega) were performed on cells 48 or 72 h after treatment with 1 μ g/mL dox according to
463 the manufacturer's instructions.

464

465 Statistical Analysis

466 Data analysis was performed with Prism 6 (Graphpad Software). Statistical significance was
467 evaluated with an unpaired *t*-test for comparison between two means and analysis of variance
468 followed by Bonferroni method for multiple comparisons. A value of $P < 0.05$ was considered
469 to denote statistical significance.

470

471 **Supporting information**

472 Supplementary figures 1-10 (Figures S1-S10), and supplementary table 1 (Table S1). The data
473 underlying this publication are available from the University of Southampton data repository,
474 or by emailing the corresponding author of this study.

475

476 **Acknowledgement**

477 The authors thank Cancer Research UK (A20185) and the Engineering and Physical Sciences
478 Research Council (EP/K503150/1) for funding this work.

479

480 **References**

- 481 [1] Darnell, J. E., Jr. (2002) Transcription factors as targets for cancer therapy, *Nat. Rev.*
482 *Cancer* 2, 740-749.
- 483 [2] Miranda, E., Nordgren, I. K., Male, A. L., Lawrence, C. E., Hoakwie, F., Cuda, F., Court,
484 W., Fox, K. R., Townsend, P. A., Packham, G. K., Eccles, S. A., and Tavassoli, A.
485 (2013) A Cyclic Peptide Inhibitor of HIF-1 Heterodimerization That Inhibits Hypoxia
486 Signaling in Cancer Cells, *J. Am. Chem. Soc.* 135, 10418-10425.
- 487 [3] Ebert, B. L., and Bunn, H. F. (1998) Regulation of transcription by hypoxia requires a
488 multiprotein complex that includes hypoxia-inducible factor 1, an adjacent
489 transcription factor, and p300/CREB binding protein, *Mol. Cell. Biol.* 18, 4089-4096.
- 490 [4] Wang, G. L., Jiang, B. H., Rue, E. A., and Semenza, G. L. (1995) Hypoxia-inducible
491 factor 1 is a basic-helix-loop-helix-PAS heterodimer regulated by cellular O₂ tension,
492 *Proc Natl Acad Sci U S A* 92, 5510-5514.
- 493 [5] Schodel, J., Oikonomopoulos, S., Ragoussis, J., Pugh, C. W., Ratcliffe, P. J., and Mole, D.
494 R. (2011) High-resolution genome-wide mapping of HIF-binding sites by ChIP-seq,
495 *Blood* 117, e207-217.
- 496 [6] Jaakkola, P., Mole, D. R., Tian, Y. M., Wilson, M. I., Gielbert, J., Gaskell, S. J.,
497 Kriegsheim, A., Hebestreit, H. F., Mukherji, M., Schofield, C. J., Maxwell, P. H.,
498 Pugh, C. W., and Ratcliffe, P. J. (2001) Targeting of HIF- α to the von Hippel-
499 Lindau ubiquitylation complex by O₂-regulated prolyl hydroxylation, *Science* 292,
500 468-472.

- 501 [7] Ivan, M., Kondo, K., Yang, H., Kim, W., Valiando, J., Ohh, M., Salic, A., Asara, J. M.,
502 Lane, W. S., and Kaelin, W. G., Jr. (2001) HIF α targeted for VHL-mediated
503 destruction by proline hydroxylation: implications for O₂ sensing, *Science* 292, 464-
504 468.
- 505 [8] Jewell, U. R., Kvietikova, I., Scheid, A., Bauer, C., Wenger, R. H., and Gassmann, M.
506 (2001) Induction of HIF-1 α in response to hypoxia is instantaneous, *FASEB J.*
507 15, 1312-1314.
- 508 [9] Keith, B., Johnson, R. S., and Simon, M. C. (2012) HIF1 α and HIF2 α : sibling
509 rivalry in hypoxic tumour growth and progression, *Nat. Rev. Cancer* 12, 9-22.
- 510 [10] Harris, A. L. (2002) Hypoxia--a key regulatory factor in tumour growth, *Nat. Rev.*
511 *Cancer* 2, 38-47.
- 512 [11] Semenza, G. L. (2003) Targeting HIF-1 for cancer therapy, *Nat. Rev. Cancer* 3, 721-732.
- 513 [12] Giaccia, A., Siim, B. G., and Johnson, R. S. (2003) HIF-1 as a target for drug
514 development, *Nat Rev Drug Discov* 2, 803-811.
- 515 [13] Bardos, J. I., and Ashcroft, M. (2004) Hypoxia-inducible factor-1 and oncogenic
516 signalling, *Bioessays* 26, 262-269.
- 517 [14] Scott, C. P., Abel-Santos, E., Wall, M., Wahnou, D. C., and Benkovic, S. J. (1999)
518 Production of cyclic peptides and proteins in vivo, *Proc Natl Acad Sci U S A* 96,
519 13638-13643.
- 520 [15] Tavassoli, A., and Benkovic, S. J. (2007) Split-intein mediated circular ligation used in
521 the synthesis of cyclic peptide libraries in *E. coli*, *Nat Protoc* 2, 1126-1133.
- 522 [16] Wu, H., Hu, Z. M., and Liu, X. Q. (1998) Protein trans-splicing by a split intein encoded
523 in a split DnaE gene of *Synechocystis* sp. PCC6803, *Proc Natl Acad Sci U S A* 95,
524 9226-9231.
- 525 [17] Lennard, K. R., and Tavassoli, A. (2014) Peptides come round: using SICLOPPS
526 libraries for early stage drug discovery, *Chemistry* 20, 10608-10614.
- 527 [18] Iwai, H., Zuger, S., Jin, J., and Tam, P. H. (2006) Highly efficient protein trans-splicing
528 by a naturally split DnaE intein from *Nostoc punctiforme*, *FEBS Lett* 580, 1853-1858.
- 529 [19] Lockless, S. W., and Muir, T. W. (2009) Traceless protein splicing utilizing evolved split
530 inteins, *Proc Natl Acad Sci U S A* 106, 10999-11004.
- 531 [20] Townend, J. E., and Tavassoli, A. (2016) Traceless Production of Cyclic Peptide
532 Libraries in *E. coli*, *ACS Chem Biol* 11, 1624-1630.
- 533 [21] Schlake, T., and Bode, J. (1994) Use of mutated FLP recognition target (FRT) sites for
534 the exchange of expression cassettes at defined chromosomal loci, *Biochemistry* 33,
535 12746-12751.
- 536 [22] Rapisarda, A., Uranchimeg, B., Scudiero, D. A., Selby, M., Sausville, E. A., Shoemaker,
537 R. H., and Melillo, G. (2002) Identification of small molecule inhibitors of hypoxia-
538 inducible factor 1 transcriptional activation pathway, *Cancer Res.* 62, 4316-4324.
- 539 [23] Cao, Y. J., Shibata, T., and Rainov, N. G. (2001) Hypoxia-inducible transgene
540 expression in differentiated human NT2N neurons - a cell culture model for gene
541 therapy of postischemic neuronal loss, *Gene Therapy* 8, 1357-1362.
- 542 [24] Post, D. E., and Van Meir, E. G. (2001) Generation of bidirectional hypoxia/HIF-
543 responsive expression vectors to target gene expression to hypoxic cells, *Gene*
544 *Therapy* 8, 1801-1807.
- 545 [25] Soderberg, O., Gullberg, M., Jarvius, M., Ridderstrale, K., Leuchowius, K. J., Jarvius, J.,
546 Wester, K., Hydbring, P., Bahram, F., Larsson, L. G., and Landegren, U. (2006)
547 Direct observation of individual endogenous protein complexes in situ by proximity
548 ligation, *Nat. Methods* 3, 995-1000.
- 549 [26] Koh, M. Y., Lemos, R., Jr., Liu, X., and Powis, G. (2011) The hypoxia-associated factor
550 switches cells from HIF-1 α - to HIF-2 α -dependent signaling promoting stem
551 cell characteristics, aggressive tumor growth and invasion, *Cancer Res* 71, 4015-
552 4027.
- 553 [27] Uchida, T., Rossignol, F., Matthay, M. A., Mounier, R., Couette, S., Clottes, E., and
554 Clerici, C. (2004) Prolonged hypoxia differentially regulates hypoxia-inducible factor

555 (HIF)-1alpha and HIF-2alpha expression in lung epithelial cells: implication of
556 natural antisense HIF-1alpha, *Journal of Biological Chemistry* 279, 14871-14878.

557 [28] Grabmaier, K., MC, A. d. W., Verhaegh, G. W., Schalken, J. A., and Oosterwijk, E.
558 (2004) Strict regulation of CAIX(G250/MN) by HIF-1alpha in clear cell renal cell
559 carcinoma, *Oncogene* 23, 5624-5631.

560 [29] Wang, Z. Q., Malone, M. H., Thomenius, M. J., Zhong, F., Xu, F., and Distelhorst, C. W.
561 (2003) Dexamethasone-induced gene 2 (dig2) is a novel pro-survival stress gene
562 induced rapidly by diverse apoptotic signals, *Journal of Biological Chemistry* 278,
563 27053-27058.

564 [30] Ellisen, L. W., Ramsayer, K. D., Johannessen, C. M., Yang, A., Beppu, H., Minda, K.,
565 Oliner, J. D., McKeon, F., and Haber, D. A. (2002) REDD1, a developmentally
566 regulated transcriptional target of p63 and p53, links p63 to regulation of reactive
567 oxygen species, *Mol Cell* 10, 995-1005.

568 [31] Maher, J. C., Wangpaichitr, M., Savaraj, N., Kurtoglu, M., and Lampidis, T. J. (2007)
569 Hypoxia-inducible factor-1 confers resistance to the glycolytic inhibitor 2-deoxy-D-
570 glucose, *Molecular Cancer Therapeutics* 6, 732-741.

571 [32] Niles, A. L., Moravec, R. A., Eric Hesselberth, P., Scurria, M. A., Daily, W. J., and Riss,
572 T. L. (2007) A homogeneous assay to measure live and dead cells in the same sample
573 by detecting different protease markers, *Anal Biochem* 366, 197-206.

574 [33] Nicholson, D. W., and Thornberry, N. A. (1997) Caspases: killer proteases, *Trends*
575 *Biochem Sci* 22, 299-306.

576 [34] Kumar, K., Wigfield, S., Gee, H. E., Devlin, C. M., Singleton, D., Li, J. L., Buffa, F.,
577 Huffman, M., Sinn, A. L., Silver, J., Turley, H., Leek, R., Harris, A. L., and Ivan, M.
578 (2013) Dichloroacetate reverses the hypoxic adaptation to bevacizumab and enhances
579 its antitumor effects in mouse xenografts, *J. Mol. Med.* 91, 749-758.

580 [35] Maher, J. C., Wangpaichitr, M., Savaraj, N., Kurtoglu, M., and Lampidis, T. J. (2007)
581 Hypoxia-inducible factor-1 confers resistance to the glycolytic inhibitor 2-deoxy-D-
582 glucose, *Mol. Cancer Ther.* 6, 732-741.

583 [36] Burroughs, S. K., Kaluz, S., Wang, D., Wang, K., Van Meir, E. G., and Wang, B. (2013)
584 Hypoxia inducible factor pathway inhibitors as anticancer therapeutics, *Future*
585 *medicinal chemistry* 5, 10.4155/fmc.4113.4117.

586 [37] Samanta, D., Gilkes, D. M., Chaturvedi, P., Xiang, L., and Semenza, G. L. (2014)
587 Hypoxia-inducible factors are required for chemotherapy resistance of breast cancer
588 stem cells, *Proc Natl Acad Sci U S A* 111, E5429-5438.

589 [38] Li, J., Shi, M. X., Cao, Y., Yuan, W. S., Pang, T. X., Li, B. Z., Sun, Z., Chen, L., and
590 Zhao, R. C. H. (2006) Knockdown of hypoxia-inducible factor-1 alpha in breast
591 carcinoma MCF-7 cells results in reduced tumor growth and increased sensitivity to
592 methotrexate, *Biochem. Bioph. Res. Co.* 342, 1341-1351.

593 [39] Sun, X., Kanwar, J. R., Leung, E., Lehnert, K., Wang, D., and Krissansen, G. W. (2001)
594 Gene transfer of antisense hypoxia inducible factor-1 alpha enhances the therapeutic
595 efficacy of cancer immunotherapy, *Gene Therapy* 8, 638-645.

596 [40] Hubbi, M. E., Kshitiz, Gilkes, D. M., Rey, S., Wong, C. C., Luo, W., Kim, D. H., Dang,
597 C. V., Levchenko, A., and Semenza, G. L. (2013) A nontranscriptional role for HIF-
598 1alpha as a direct inhibitor of DNA replication, *Sci Signal* 6, ra10.

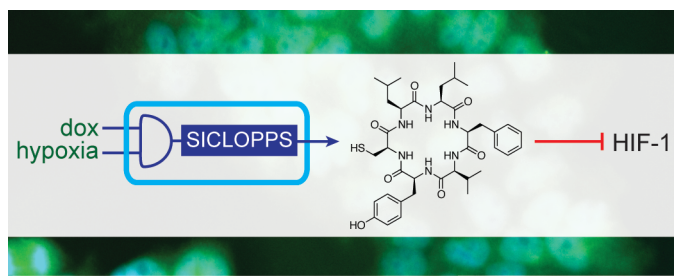
599 [41] Johns, R. A., Takimoto, E., Meuchel, L. W., Elsaigh, E., Zhang, A., Heller, N. M.,
600 Semenza, G. L., and Yamaji-Kegan, K. (2016) Hypoxia-Inducible Factor 1alpha Is a
601 Critical Downstream Mediator for Hypoxia-Induced Mitogenic Factor
602 (FIZZ1/RELMalpha)-Induced Pulmonary Hypertension, *Arterioscler Thromb Vasc*
603 *Biol* 36, 134-144.

604 [42] Xiang, L., Gilkes, D. M., Hu, H., Luo, W., Bullen, J. W., Liang, H., and Semenza, G. L.
605 (2015) HIF-1alpha and TAZ serve as reciprocal co-activators in human breast cancer
606 cells, *Oncotarget* 6, 11768-11778.

607 [43] Slomovic, S., and Collins, J. J. (2015) DNA sense-and-respond protein modules for
608 mammalian cells, *Nat Methods* 12, 1085-1090.

- 609 [44] Chan, C. T., Lee, J. W., Cameron, D. E., Bashor, C. J., and Collins, J. J. (2016)
610 'Deadman' and 'Passcode' microbial kill switches for bacterial containment, *Nat Chem*
611 *Biol* 12, 82-86.
- 612 [45] Galloway, K. E., Franco, E., and Smolke, C. D. (2013) Dynamically reshaping signaling
613 networks to program cell fate via genetic controllers, *Science* 341, 1235005.
- 614 [46] Heng, B. C., Aubel, D., and Fussenegger, M. (2015) Prosthetic gene networks as an
615 alternative to standard pharmacotherapies for metabolic disorders, *Curr Opin*
616 *Biotechnol* 35, 37-45.
- 617 [47] Kojima, R., Aubel, D., and Fussenegger, M. (2015) Novel theranostic agents for next-
618 generation personalized medicine: small molecules, nanoparticles, and engineered
619 mammalian cells, *Curr Opin Chem Biol* 28, 29-38.
- 620 [48] Morsut, L., Roybal, K. T., Xiong, X., Gordley, R. M., Coyle, S. M., Thomson, M., and
621 Lim, W. A. (2016) Engineering Customized Cell Sensing and Response Behaviors
622 Using Synthetic Notch Receptors, *Cell* 164, 780-791.
- 623 [49] Roybal, K. T., Rupp, L. J., Morsut, L., Walker, W. J., McNally, K. A., Park, J. S., and
624 Lim, W. A. (2016) Precision Tumor Recognition by T Cells With Combinatorial
625 Antigen-Sensing Circuits, *Cell* 164, 770-779.
- 626 [50] Saxena, P., Charpin-El Hamri, G., Folcher, M., Zulewski, H., and Fussenegger, M.
627 (2016) Synthetic gene network restoring endogenous pituitary-thyroid feedback
628 control in experimental Graves' disease, *Proc Natl Acad Sci U S A* 113, 1244-1249.
629
630

631 TOC graphic



632